

Calcium-Alginate-Chitosan의 스트론튬 이온 흡착 거동

Dong Lan[†], Deng Bing, Ding Lanlan, Cheng Qiong, Yang Yong, and Du Yang

Institute of Nuclear Physics and Chemistry, China Academy of Engineering Physics
(2013년 12월 15일 접수, 2014년 3월 21일 수정, 2014년 4월 20일 채택)

Adsorption Behavior of Sr Ion on Calcium-Alginate-Chitosan

Dong Lan[†], Deng Bing, Ding Lanlan, Cheng Qiong, Yang Yong, and Du Yang

Institute of Nuclear Physics and Chemistry, China Academy of Engineering Physics, Mianyang 621900, China
(Received December 15, 2013; Revised March 21, 2014; Accepted April 20, 2014)

Abstract: Sodium alginate and chitosan are added to a CaCl₂ solution to prepare calcium-alginate-chitosan and calcium-alginate gels. After dehydration through stoving, two types of adsorbent particles are obtained. The adsorption process of the particles obtained for low concentrations of Sr²⁺ satisfies a second-order kinetic equation and the Freundlich adsorption model. The thermodynamic behaviors of the particles indicate that adsorption occurs via a spontaneous physical process. XPS pattern analysis is used to demonstrate the adsorption of Sr²⁺ by calcium alginate and chitosan. By building an interaction model of the molecules of chitosan and alginate with Ca²⁺ and Sr²⁺ to calculate energy parameters, Fukui index, Mulliken charge, and Mulliken population, adsorption of Sr²⁺ on the molecular chains of chitosan as well as the boundary of calcium-alginate-chitosan is observed to show weak stability; by contrast, adsorption between molecular chains is high.

Keywords: Ca-alginate-chitosan, adsorption, Sr²⁺, kinetics, thermodynamics.

Introduction

⁹⁰Sr is a key nuclide in fission and an important index in environmental monitoring. The use of radiochemical analysis to isolate ⁹⁰Sr in purified water as well as α - and β -low-background measuring instruments to measure β radioactivity are common practices. However, in the early stages of research, ⁹⁰Sr isolation is a time-consuming, complicated, and laborious process. Numerous local and foreign researchers continue to search for materials with the maximum capacity to eliminate interference elements. While United States standards (2008)¹ specify the use of crown-ether-Sr resin to isolate ⁹⁰Sr, Chinese researchers have not fully mastered the method for synthesizing materials used for ⁹⁰Sr isolation and material costs are usually very high. Therefore, research of synthesis methods for low-cost and highly efficient isolation and adsorption materials is of great significance.

Chitin [(1,4)-2-amino-2-deoxy- β -D-glucan] is a natural cationic polymer derived from chitosan through a deacetylation

reaction. The N atoms on the amino group of the molecular chain provide a lone electron pair, converting chitosan into a charged electrolyte that has excellent adsorption capacity for heavy metal ions. Despite the number of adsorption studies currently available, the poor mechanical properties of chitosan have limited its application as an adsorbent. Alginate, a natural polysaccharide isolated from brown algae, is a copolymer made up of different amounts of β -D mannuronic acid (M) residues and its epimer, α -L guluronic acid (G).^{2,3} The molecular structure of alginate contains a large number of hydroxy groups and carboxyl groups. The negative charge carried by the hydroxy group and the positive charge carried by metal ions allow the groups to combine into a gel due to electrostatic attraction, the underlying mechanism of which has been demonstrated to resemble an "egg-box" model.⁴ The carboxyl group of alginate and the amino group of chitosan can form an adsorbent that integrates the advantages of both polymers. Research shows that the bonded adsorbent not only has excellent adsorption performance for metal ions but also possesses ideal mechanical properties, which satisfies the needs for preparation and application. Numerous studies⁵⁻⁷ report the rapid adsorption of metal ions, such as Cu²⁺, Cd²⁺, and Ni²⁺, by chi-

[†]To whom correspondence should be addressed.
E-mail: shuangyusuchi@163.com

tosan. However, studies on the joint adsorption of Sr^{2+} by calcium alginate and chitosan have yet to be reported. To study the behavior and mechanism of Sr^{2+} adsorption by calcium-alginate–chitosan, we explore the adsorption kinetics and thermodynamics of two adsorbents and use Materials Studio 5.0 software to calculate the energy necessary for chitosan and alginate block molecules to react with Ca^{2+} and Sr^{2+} . We propose an adsorption mechanism that could serve as a foundation for future research on the isolation of ^{90}Sr .

Experimental

Materials. Alginate, chitosan, strontium nitrate, barium chloride, hydrochloric acid and sodium hydroxide used in this experiment were all analytical reagents and they were purchased from Aladdin Co. Ltd., China.

Preparation of Calcium-Alginate–Chitosan and Calcium Particles. Solutions of sodium alginate solution (10 g/L) and mixed alginate and chitosan (10 g/L) were prepared. The solutions were added dropwise into a CaCl_2 solution of the same concentration to prepare calcium alginate and calcium-alginate–chitosan gel beads. The addition process was completed with magnetic stirring at 400 rpm. Deionized water was used to remove extra calcium ions from the gel beads. The gel beads were dried at 120 °C and ground to 40 mesh for later use. All glassware was ultrasonically cleaned. The products were immersed in 5% HNO_3 for 24 h, cleaned with deionized water, immersed in 5% NaOH for 24 h, and then cleaned repeatedly with deionized water.

Adsorption Behavior of Calcium Alginate and Calcium-Alginate–Chitosan on Sr^{2+} . **Adsorption Kinetics Experiment:** About 0.2 g of preprocessed calcium alginate and calcium-alginate–chitosan particles were placed in a beaker and mixed with 100 $\mu\text{g/L}$ Sr^{2+} solution. The solution was left to stand for 24 h. An atomic adsorption spectrometer (AAS Zeenit 700P Germany) was used to measure the ion concentration at short time intervals. Then, based on the difference between the component concentration before and after the adsorption, adsorption was calculated ($\mu\text{g/g}$) and the kinetics curve was plotted.

Adsorption Thermodynamics Experiment: At temperatures of 20, 30, and 40 °C, 0.2 g of calcium alginate and calcium-alginate–chitosan particles were weighed and added to separate beakers. Ten milliliters of Sr^{2+} solution was poured into the beaker. After the solution had been left to stand for 24 h at room temperature, we determined the ion concentration and plotted the static isothermal adsorption curve to calculate

thermodynamic parameters.

XPS Characterization Before and After Adsorption: After complete drying, the sample was packaged following oxygen plasma treatment for XPS analysis. Wide-band scanning was performed from 0 to 1100 eV at a step size of 1 eV.

Exploration of Adsorption Mechanism. Modeling and Simulation of Alginate–Chitosan: Based on two types of chitosan monomers, M and G, we built double-polymer chains with a polymerization degree of $n=2$. Four models of atactic and alternative copolymers were established, including chitosan single-stranded molecules (denoted as 2C), chitosan double-stranded molecules (denoted as 4C), alginic-acid-block double-stranded molecules (denoted as 2GM), and chitosan–alginic-acid-block double-stranded molecule (denoted as 2C-GM). H-terminal blocking was adopted for all polymer chains. We used Discover COMPASS force field in Materials Studio 5.0 to conduct Minimizer optimizing calculations for the polymer models with a total of 2000 steps. Then, NVT ensemble and Nose constant-temperature calculations were employed to conduct molecular dynamics simulations at 298 K for 1 fs. The calculation reached system equilibrium.

Modeling and Calculation for the Reaction of Alginate Block Molecules with Ca^{2+} and Sr^{2+} : Based on the Adsorption module, we applied Monte Carlo simulation to search for the low-energy action site of Ca^{2+} and Sr^{2+} on alginate block molecules. Then, based on the QMERA module, the hybrid QM/MM method was used to study the energy and electron properties of alginate's reaction with Ca^{2+} and Sr^{2+} ; thus, we explored the mechanism of Sr^{2+} adsorption by calcium alginate. We used the quantum mechanics (QM) DMol³ module for metal ions and O atoms that are potentially involved in the reaction.⁸ According to the fully electric density functional theory, generalized gradient approximation was adopted for the fitting and electron exchange-correlation functional PW91. By taking into account relativistic effects and performing full-electronic calculations with the DNP basis set, higher precision may be expected. Convergence precision was preset as fine, that is, the energy change in each atom in the convergence was less than 1.0×10^{-4} eV/nm and the energy gradient change was less than 2.0×10^{-3} . Excluding Ca^{2+} , Sr^{2+} , and some O atoms, the rest of the atoms were calculated with the molecular mechanics (MM) GULP module, and the energy was calculated with a universal force field. Calculations of the energy and electroproperties for the reaction of alginate block molecules with Ca^{2+} and Sr^{2+} included those for the QM/MM energy, the maximum occupying orbital energy level, the Fukui index, and the

Mulliken charge distribution.

Results and Discussion

Kinetic Properties of Adsorption. Studies of models for adsorption kinetics can help elucidate possible reaction mechanisms and predict reaction rates. The pseudo-first-order kinetic and pseudo-second-order kinetic models were established.⁹ The model describing the pseudo-first-order kinetic model can be expressed as:

$$\log(Q_e - Q) = \log Q_e - k_1 \frac{t}{2.303} \tag{1}$$

where $Q(\text{mg/g})$ is the adsorption quantity of resin at t , $Q_e(\text{mg/g})$ is the saturated adsorption quantity of resin, $t(\text{h})$ is the adsorption time, and k_1 is the pseudo-first-order adsorption rate constant. We used Origin 8.0 software to perform linear fitting for t with $\log(Q_e - Q)$ on the vertical coordinate and obtained a pseudo-first-order kinetic model, as shown by (a) in Figure 1. Moreover, k_1 and Q_e can be calculated from the slope and intercept in (a). We obtained a pseudo-second-order kinetic model, which can be expressed by the following formula:

$$\frac{t}{Q} = \frac{1}{k_2 Q_e^2} + t Q_e \tag{2}$$

where k_2 is the pseudo-second-order adsorption rate constant. The pseudo-second-order kinetic model obtained through linear fitting for t/Q is shown in (b) of Figure 1. k_2 and Q_e were calculated from the slope and intercept of (b). Refer to Table 1 for the equation parameters.

Figure 1 and Table 1 show that the first- and second-order-adsorption kinetic models for calcium-alginate-chitosan and calcium alginate demonstrate good linear correlation. Since the second-order adsorption kinetic model shows more linear results, the adsorption kinetic process can be better described by it. The adsorption process in the solution is quite complicated, and comparison of the adsorption quantity of the two kinds of particles indicates that calcium-alginate-chitosan has slightly higher adsorption quantity than calcium alginate. Under acidic conditions, Sr^{2+} is more likely to diffuse to the surface of calcium-alginate-chitosan and calcium alginate and more likely to form coordinate and ionic bonds.

Thermodynamic Study on Resin Adsorption. Based on the adsorption equilibrium study on the adsorption isotherm model and thermodynamic parameters, the aim of the thermodynamic study on calcium-alginate-chitosan and calcium alginate is to evaluate the effect of temperature on the adsorption capacity of the adsorbent. The properties of the surface of the adsorbent are determined by the adsorption equilibrium constant. To better understand the adsorption mechanism for

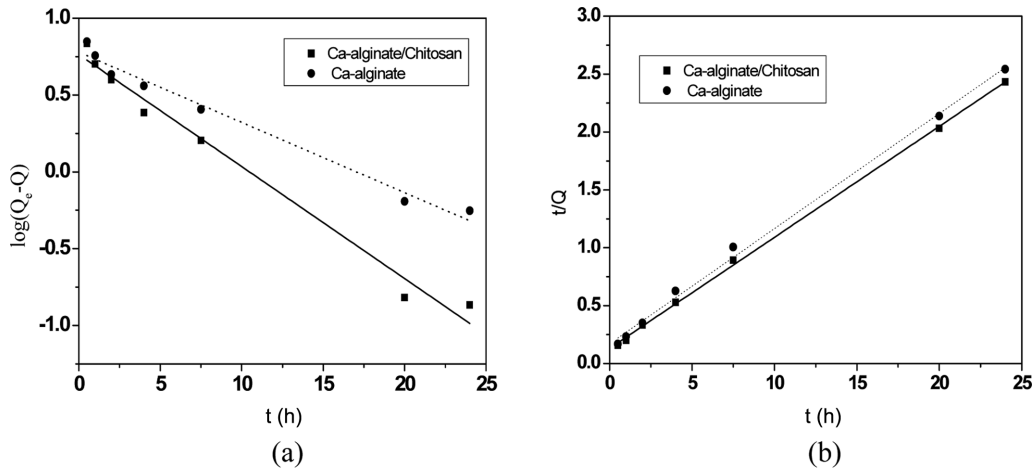


Figure 1. Kinetic curves for Sr^{2+} adsorption by calcium-alginate-chitosan and calcium alginate: (a) first-order kinetics; (b) second-order kinetics.

Table 1. Adsorption-Kinetic-Model Parameters for Calcium-Alginate-Chitosan and Calcium Alginate

Type	First-order kinetic model			Second-order kinetic model		
	$Q_e(\text{mg/g})$	k_2	R^2	$Q_e(\text{mg/g})$	k_2	R^2
Calcium-alginate-chitosan	5.7982	0.1679	0.9802	10.4297	0.0699	0.9992
Calcium alginate	6.0113	0.1053	0.9782	10.0624	0.0576	0.9964

the two kinds of Sr^{2+} particles, we used two classical models, the Langmuir model and the Freundlich model, for fitting with the experimental data. As an ideal monomolecular-layer adsorption model, the Langmuir model presumes that adsorption occurs under the condition of particle surface uniformity and equal adsorption capacity of the particles. The Langmuir isothermal adsorption model can be expressed by the following equation:

$$Q_e = \frac{QC}{k_d + C} \tag{3}$$

Eq. (3) is transformed to:

$$\frac{C}{Q_e} = \frac{k_d}{Q} + \frac{C}{Q} \tag{4}$$

where $Q_e(\text{mg/g})$ is the adsorption quantity in the equilibrium state, $Q(\text{mg/g})$ is the saturated adsorption quantity, $C(\text{mg/L})$ is the concentration of $\text{Sr}(\text{NO}_3)_2$, $t(\text{h})$ is the adsorption time, and k_d is the effective dissociation constant. By conducting linear

fitting for C using Origin 8.0 software with C/Q as the vertical coordinate, we obtained Langmuir isothermal adsorption models for calcium-alginate-chitosan and calcium alginate at three temperatures, as shown by (a) in Figures 2 and 3. Equation parameters k_d and Q are calculated with the slope and intercept in (a). Results are shown in Tables 2 and 3. The Freundlich adsorption model can be applied to the heterogeneous surface of the adsorbent, and its equation may be written as:

$$Q = k_F C^{\frac{1}{n}} \tag{5}$$

Taking the logarithm of both sides of eq. (5):

$$\log Q = \log k_F + \frac{1}{n} \log C \tag{6}$$

where k_F is the Freundlich adsorption coefficient and n is the Freundlich constant. The rest of the variables are identical to those in eq. (4). By plotting $\log C$ vs. $\log Q$, we can obtain the Freundlich isothermal adsorption model for the two types of

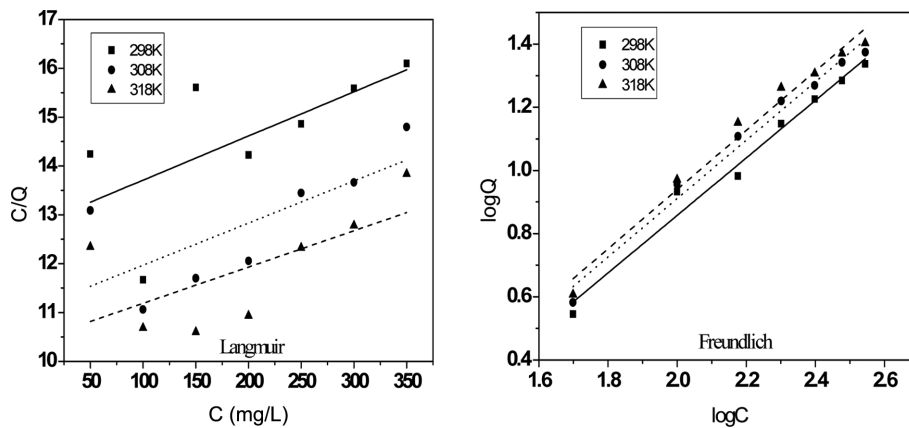


Figure 2. Isothermal adsorption curves for calcium-alginate-chitosan on Sr^{2+} .

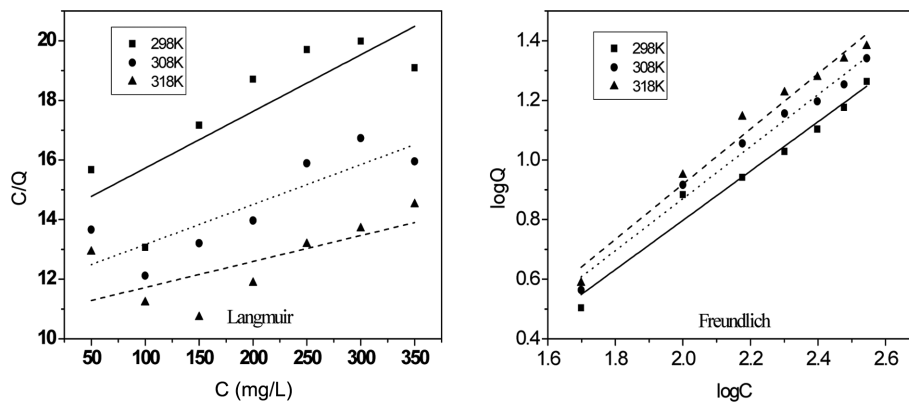


Figure 3. Isothermal adsorption curves for calcium alginate on Sr^{2+} .

Table 2. Langmuir and Freundlich-Isothermal-Adsorption Parameters

$T(K)$	Langmuir equation			Freundlich equation			
	$Q(mg/g)$	k_d	R^2	$k_f(mg/g)$	N	R^2	
Calcium-alginate-chitosan	298	110.50	1415.0	0.3217	0.1087	1.0980	0.9760
	308	115.87	1286.9	0.4238	0.1153	1.0816	0.9779
	318	134.59	1405.7	0.3148	0.1161	1.0668	0.9755
Calcium alginate	298	52.580	726.83	0.6004	0.1392	1.2093	0.9654
	308	74.570	881.50	0.6717	0.1334	1.1461	0.9792
	318	114.68	1244.2	0.3673	0.1167	1.0800	0.9723

adsorbents, as shown in Figures 2 and 3. The equation's slope and intercept are $1/n$ and $\log k_f$, respectively. Relevant model parameters are shown in Table 2.

Adsorption Thermodynamic Properties of Calcium Alginate. Figures 2 and 3 show the isothermal adsorption curves for calcium-alginate-chitosan and calcium alginate on Sr^{2+} at different temperatures. As coefficients in the Freundlich equation, n and k_f can reflect the adsorption amount, as shown in Table 2. The k_f value reached its maximum at 298 K and decreased with increasing temperature. At this point, $n > 1$, which indicates that Sr^{2+} adsorption by calcium alginate has certain advantages at low temperature. The Van't Hoff plot (Figure 4) shows linear correlation.

The data in Figure 2, Figure 3, and Table 2 show that all of the correlation coefficients of the Freundlich model for Sr^{2+} adsorption by calcium-alginate-chitosan and calcium alginate are greater than those of the Langmuir model. Thus, the entire process involves a heterogeneous surface, and the Freundlich model can properly describe the adsorption process. The $1/n$ of the two types of resin varies between 0.82 and 0.94, well within the range of easy adsorption.

According to the Van't Hoff equation, the isosteric heat of

adsorption for calcium-alginate-chitosan and calcium alginate on Sr^{2+} can be deduced by the simultaneous solution of $d \ln K / dT = \Delta H / RT^2$ and the Freundlich equation. Based on the isothermal adsorption data shown in Figure 4, we can calculate ΔH from the slope obtained through plotting of $1/T$ vs. $\ln K$. According to the Gibbs equation, we obtain the free-energy change of adsorption by the equation $\Delta G = -RT \int_0^C (q_e/c_e) dc_e$. When the latter equation is combined with the Freundlich equation, the equation $\Delta G = -nRT$ will be obtained, where n is the Freundlich equation parameter in Table 1. ΔS is given by $\Delta S = (\Delta H - \Delta G) / T$. Refer to Table 3 for the results.

Table 3 shows that the isosteric adsorption enthalpy for calcium-alginate-chitosan on Sr^{2+} is positive, whereas the value for calcium alginate is negative. Some differences in the adsorption performance of the two adsorbents in low-concentration Sr^{2+} solution may be observed, but the absolute values for the two adsorbents are relatively small, which indicates that the adsorption process is a physical one. The ΔG value for both adsorbents is < 0 , which suggests the spontaneity of adsorption. The entropy ΔS is positive, which shows that, under the effect of absorptive forces, Sr^{2+} passes through calcium alginate particles to enter inside until the attachment is

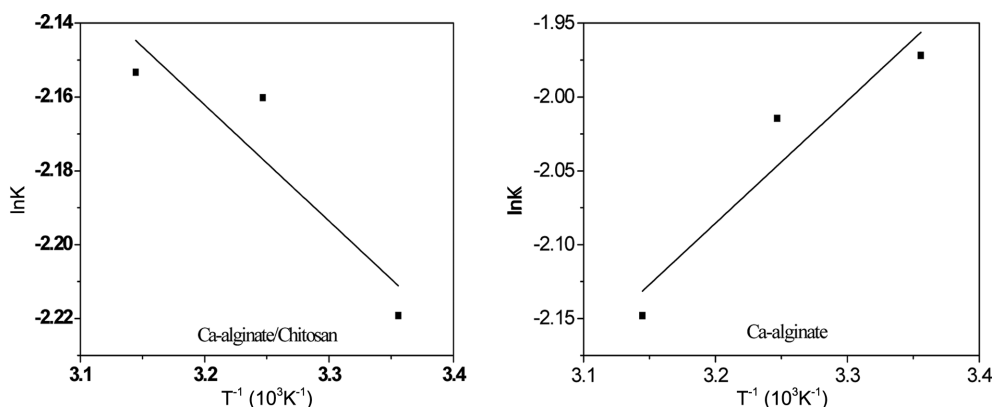
**Figure 4.** Van't Hoff plots showing linear relations.

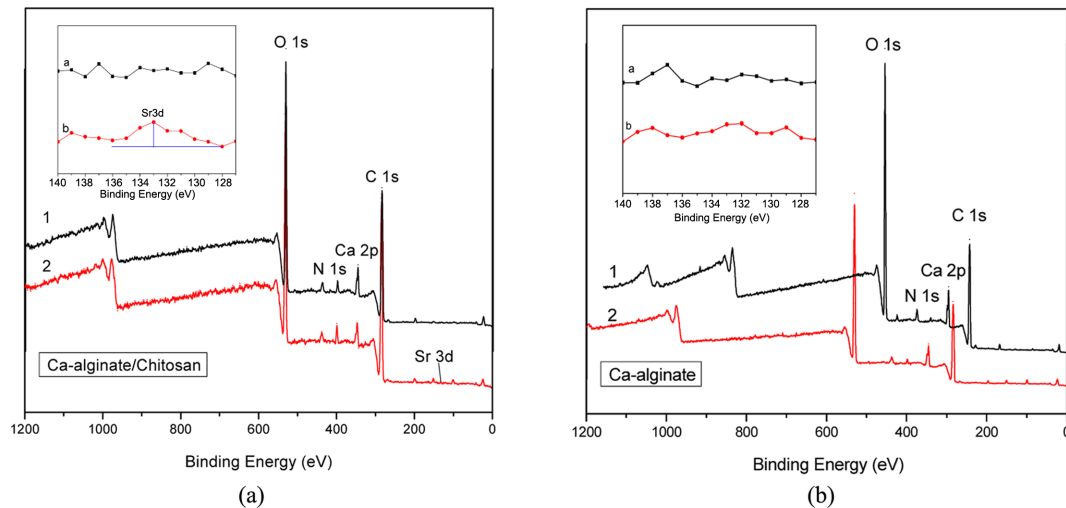
Table 3. Thermodynamic Parameters for the Adsorption of Calcium-Alginate–Chitosan and Calcium Alginate

	$T(K)$	$\ln K$	$\Delta G(kJ/mol)$	$\Delta H(kJ/mol)$	$\Delta S(kJ(mol/K))$
Calcium-alginate–chitosan	298	-2.2192	-2.7204		0.0091
	308	-2.1602	-2.7697	0.0026	0.0090
	318	-2.1533	-2.8205		0.0089
Calcium alginate	298	-1.9718	-2.9961		0.0100
	308	-2.0144	-2.9348	-0.0069	0.0095
	318	-2.1482	-2.8554		0.0090

more vigorous than in the solvent. The whole system becomes more disordered and the adsorption becomes more random.

Figure 5 shows the XPS patterns before and after adsorption of Sr^{2+} by calcium-alginate–chitosan and calcium alginate. Curves 1 and 2 represent the status before and after adsorption,

respectively. The graph shows a distinct main peak for calcium. Elemental Sr is captured on the surface of calcium-alginate–chitosan (Figure 5(a)), and a very small 3D peak appears at 133 eV. However, no peak is observed for the binding energy on the surface of calcium alginate after adsorption (Fig-

**Figure 5.** XPS patterns obtained before and after the adsorption of Sr^{2+} by calcium-alginate–chitosan and calcium alginate.**Table 4. Energy Parameters for the Different Types of Molecules**

System	QM(eV)	MM(eV)	Total energy(eV)	HOMO(eV)	LUMO(eV)	$E_{gap}(eV)$	Occupation of HOMO	Occupation of LUMO
2CCa	-16.894	17.792	0.898	4.046	4.383	0.337	0.881	0.384
2CSr	-11.580	10.395	-1.186	0.686	0.926	0.240	0.767	0.361
2CCaSr	-17.717	17.727	0.009	-3.857	-3.457	0.400	0.838	0.214
4CCa	-4.794	17.941	13.147	12.865	13.208	0.343	0.816	0.262
4CSr	-5.414	17.928	12.514	12.527	12.944	0.417	0.851	0.211
4CCaSr	-25.093	12.133	12.959	9.044	9.543	0.499	0.903	0.192
2GMCa	0.658	81.616	82.674	-9.305	-8.998	0.307	0.736	0.226
2GMSr	0.237	92.390	92.627	-8.699	-8.554	0.145	0.593	0.334
2GMCaSr	-13.958	87.468	73.510	9.266	10.018	0.752	0.952	0.073
2C-GMCa	-18.357	48.127	29.770	7.107	7.638	0.531	0.552	0.024
2C-GMSr	-18.680	53.263	34.583	6.843	7.393	0.55	0.550	0.021
2C-GMCaSr	-26.146	34.394	8.249	-0.979	-0.523	0.456	0.885	0.212

ure 5(b)). Adsorption clearly occurs when the concentration of the Sr solution is 100 $\mu\text{g/L}$, corresponding to the detection limit of the XPS spectrometer. The characteristic main peak of Sr on the surface of calcium-alginate-chitosan suggests some adsorption behavior and the higher adsorption capacity of calcium-alginate-chitosan than calcium alginate.

Exploration of Adsorption Mechanism. We used Monte Carlo simulation to search for low-energy action sites on chi-

tosan, alginate GM block, and calcium-alginate-chitosan molecules on Ca^{2+} and Sr^{2+} . From Table 4, the interaction of electrons of the two adsorbents with metal ions was calculated, with results showing some nonlocality. The probability of electrons appearing on the lowest unoccupied molecular orbital (LUMO) is around 1/3. Figure 6 shows a single strand of the chitosan 2C molecular system. The energy gap in 2C's interaction with the two metals is slightly larger than that observed

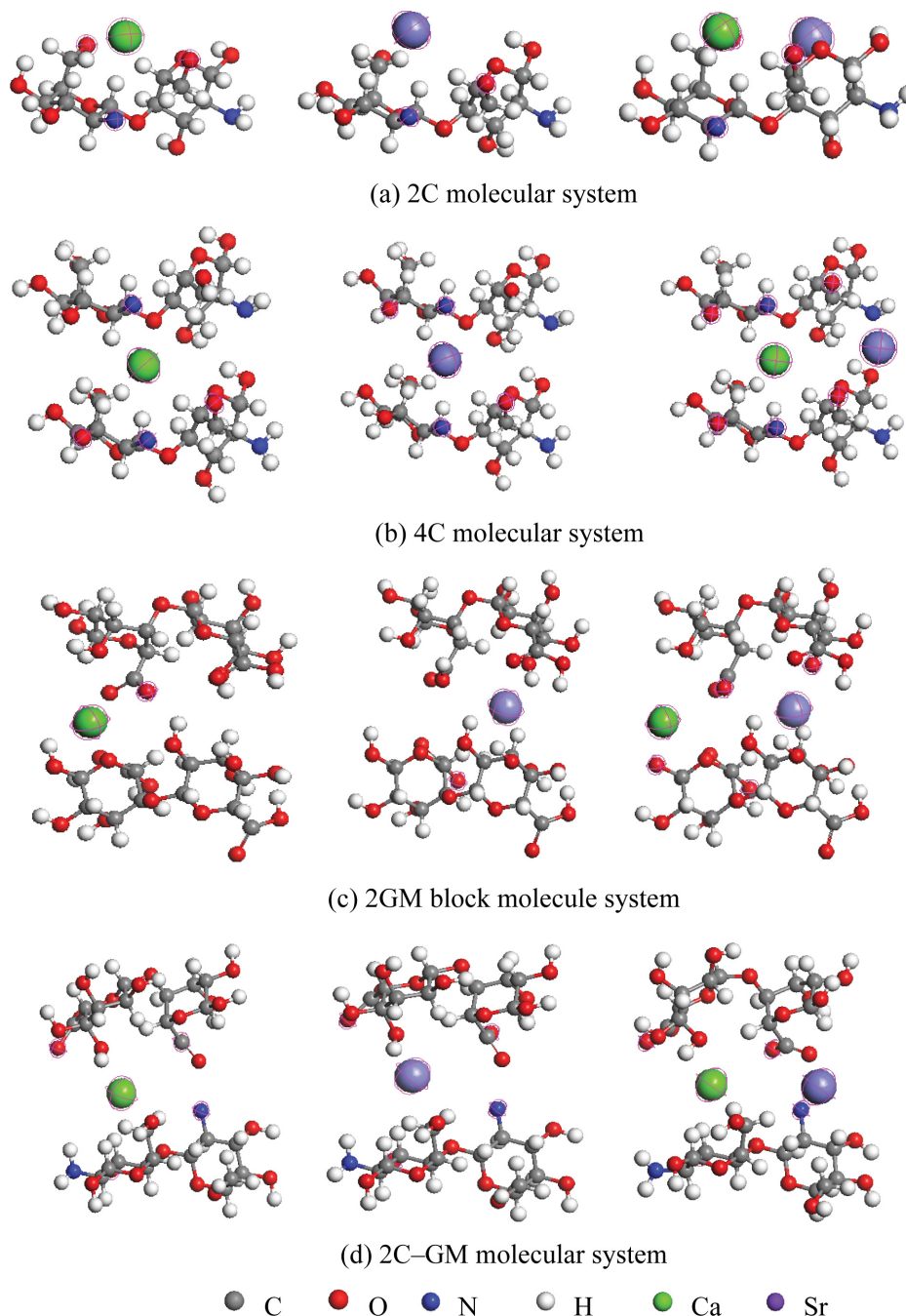


Figure 6. Alginate acid molecule GG, MM, and GM block interactions with Ca^{2+} and Sr^{2+} .

during its interaction with a single metal, but comparison of the energy gap and occupation state data indicates that the action force between 2C and Ca^{2+} and Sr^{2+} is lower than that of the three other systems, 4C, 2GM, and 2C-GM. According to the Jellium model,⁹ the amplitude of energy gap reflects chemical inertness, and the rise in stability is characterized by the decrease in the LUMO state. Thus, the adsorption of Sr^{2+} within single-stranded chain molecules can be inferred to be weaker than that between double-stranded molecules. The N obtained by the Sr ion or the electron supplied by O is very likely to escape from the outer layer, thus losing electrons and dissociating from the 2C system again. The 4C and 2GM molecular systems contain the double-chain structure of the same molecule (as shown in Figures 6(b) and 6(c)). The adsorption of Ca^{2+} and Sr^{2+} causes the energy gap in the two systems to become greater than that observed during interaction with a single kind of ion. The value of the LUMO state is small, particularly for 2GMCaSr (0.073). HOMO orbital electron delocalization is weak, thereby facilitating electron movement. Moreover, the system stability of chitosan and calcium alginate is greatly strengthened after the adsorption of Sr^{2+} . The 2C-GM system design simulates a chitosan single strand and a single strand of calcium alginate GM block (as shown in Figure 6(d)). The energy gap for 2C-GMCaSr is lower than that for 2C-GMCA and 2C-GMSr and the LUMO state value significantly rises, which suggests the stronger trend of donating electrons. Thus, when the metal ion comes into contact with the boundary of the two types of calcium-alginate–chitosan molecules, the progress of adsorption is hindered.

With the Fukui index,¹⁰ we can evaluate the nucleophilic or electrophilic properties of the active region of a molecule to determine the location and strength of its chemical activity. The Fukui index $f(r)$ is defined as the first-order partial derivative of electron number N with respect to electron density $\rho(r)$ under a given external potential field $V(r)$: $f(r) = (\partial \rho(r) / \partial N)_{V(r)}$. A finite differential approximation is performed. The Fukui function for the convergence $f(r)$ is expressed as: $f(r)^+ = q_i(N+1) - q_i(N)$ and $f(r)^- = q_i(N) - q_i(N-1)$, where $q_i(N)$, $q_i(N+1)$, and $q_i(N-1)$ represent the charge carried by atoms in molecules i when the molecules are neutrals, cations, and anions, respectively; $f(r)^+$ and $f(r)^-$ are the nucleophilic attack and electrophilic attack indices, which represent the ability of the atoms in molecules i to gain and lose electrons, respectively. Higher $f(r)^+$ and $f(r)^-$ values indicate higher ability to gain and lose electrons.

Table 5. Fukui Index of the System

System	Atom	$f(r)^+$	$f(r)^-$
2CCaSr	Ca	0.273	0.277
	Sr	0.476	0.458
4CCaSr	Ca	0.301	0.297
	Sr	0.134	0.130
2GMCaSr	Ca	0.367	0.358
	Sr	0.257	0.245
2C-GMCAr	Ca	0.229	0.220
	Sr	0.338	0.350

Table 5 compares the Fukui indices of the two types of metal ions in 2CCaSr, 4CCaSr, 2GMCaSr, and 2C-GMCAr. During simulation, molecules in the four systems are combined with Ca, after which adsorption of Sr is calculated. Comparison of the index values for Sr and Ca suggests that $\text{Sr} > \text{Ca}$ and outer electrons of Sr are active in 2CCaSr, thereby facilitating the gain and loss of electrons. Nucleophilic and electrophilic attack abilities are also suggested. The adsorption stability of this system is lower than that of the three other systems, which corresponds to the energy parameter analysis results in Table 3. The outer electrons of 4CCaSr and 2G-MCAr become less active, indicating difficulty in their transfer. By contrast, 2C-GMCAr's ability to gain and lose electrons and chemical activity become stronger and are accompanied by decreasing adsorption stability. Thus, the instability of Sr adsorption by calcium-alginate–chitosan on the boundary is also demonstrated.

The Mulliken charge and Mulliken population reflect the status of charge distribution in the adsorption by calcium alginate and calcium-alginate–chitosan. According to Table 6, the atom is the QM atom in Figure 6. After 2C molecules adsorb Sr^{2+} , the charges of the electron donors N and O decrease by varying degrees. The positive charge of Sr decreases from 2 to 0.647, which suggests that Sr and 2C interact to consume some electric charge. When Sr is introduced into the 4C and 2GM systems, the electric charge of Sr becomes negative, which suggests that the acting force produced by the system is significantly stronger than the adsorption capacity of the inside of 2C molecules on Sr. Adsorption increases the stability of the system, which is consistent with the energy parameter analysis results presented above. In 2C-GM, the electric charge of Sr decreases from 2 to 0.07, and its acting force on Sr is only slightly higher than the 2C system. Since the selection of the basis set has an enormous impact on the value of electric

Table 6. Analysis of Mulliken Charge and Mulliken Population of the System

System	2CCa	2CCaSr	4CCa	4CCaSr	2GMCa	2GMCaSr	2C-GMCa	2C-GMCaSr
N1	-0.709	-0.413	-0.815	-0.691	–	–	-0.714	-0.500
N2	–	–	-1.169	-0.640	–	–	–	–
O1	-0.902	-0.816	-1.069	-0.962	-0.398	-1.005	-1.001	-0.794
O2	-0.934	-0.755	-1.037	-0.895	–	-0.940	-0.925	-0.758
O3	–	–	–	-0.939	–	-1.041	-0.988	-0.806
O4	–	–	–	-0.943	–	-1.063	–	–
H1	0.127	0.173	0.141	0.175	0.269	0.100	0.147	0.193
H2	0.176	0.210	0.054	0.099	–	0.167	0.168	0.212
H3	0.202	0.225	0.102	0.175	–	0.177	0.074	0.146
H4	–	–	0.001	0.157	–	0.191	0.154	0.195
H5	–	–	–	0.108	–	–	–	–
H6	–	–	–	0.175	–	–	–	–
Ca	0.040	0.730	-0.206	0.457	1.129	-0.370	-0.015	0.941
Sr	–	0.647	–	-0.375	–	-0.317	–	0.071

charge, some scholars believe that the calculation is not particularly significant. However, understanding the charge transfer of atomic orbitals with the help of atomic orbital populations and determining the strength of active forces inside the molecules by comparison of the interactions of homologous molecules have important reference value.

Conclusions

The block vacancy formed by lone-pair electrons on the N atom of chitosan and alginate block molecules relies on coordination bonds and the “egg box” effect to adsorb Sr^{2+} . After gel preparation and dehydration through stoving, we derived two types of adsorbent particles. We selected classical models, the first- and second-order kinetic models, as well as the thermodynamic Langmuir and Freundlich models, to describe the mechanics of Sr^{2+} adsorption by the two adsorbents. Results show that the first-order kinetic and Freundlich models fit the adsorption process well. Thermodynamic parameters show that adsorption occurs via a spontaneous physical process. Model calculations for the interaction of chitosan and alginate molecules with Ca^{2+} and Sr^{2+} can facilitate understanding of the changes in the energy parameters and ability to gain and lose electrons. Charge transfers are clearly presented, and the adsorption mechanism can be preliminarily postulated based these transfers. Calculation results indicate that the adsorption of Sr^{2+} shows weak stability while the adsorption between

molecular chains shows strong adsorption ability within the molecular chain of chitosan and on the boundary of calcium-alginate–chitosan. Because of its low cost and ideal adsorption performance, calcium-alginate–chitosan can be applied in the measurement of ^{90}Sr as an alternative material for the adsorption and isolation of Sr^{2+} .

Acknowledgements: The fund for cultivated the youth of Institute of Nuclear Physics and Chemistry (Project No. 2011QP02) is grateful for supporting this research.

References

1. ASTM D5811-08, Standard Test Method for Strontium-90 in Water.
2. A. M. Yakup, B. M. Gülay, and Y. Meltem, *J. Hazard. Mater.*, **B109**, 191 (2004).
3. N. Ertugay and Y. K. Bayhan, *J. Hazard Mater.*, **154**, 432 (2008).
4. T. A. Davis, B. Vlesky, and A. A. Mucci, *Water Research*, **37**, 4311 (2003).
5. M. Monier, D. M. Ayad, and D. A. Abdel, *Colloid Surface B*, **94**, 250 (2012).
6. W. S. Wan, S. A. Ghani, and A. Kamari, *Bioresource Technol.*, **96**, 443 (2005).
7. M. M. Beppu, E. J. Arruda, and R. S. Vieira, *J. Membrane Sci.*, **240**, 227 (2004).
8. B. Delley, *J. Chem. Phys.*, **92**, 508 (1990).
9. N. Ertugay and Y. K. Bayhan, *J. Hazard. Mater.*, **154**, 432 (2008).
10. W. A. De, *Rev. Mod. Phys.*, **65**, 611 (1993).